STRESS FIELD IN A SPHERE
SUBJECTED TO LARGE DEFORMATIONS

T. L. CHEN† and A. J. DURELLI‡

Civil and Mechanical Engineering Department,
The Catholic University of America, Washington, D.C. 20017, U.S.A.

Abstract—The previously obtained strain fields in a sphere subjected to large deformations were converted into stress fields by using two different approaches: the strain–energy function and the concept of natural stress. Complete determination of stresses on the equatorial plane and on a plane parallel to it are given. The deviatoric stresses on the equatorial plane and the maximum shear stresses along the vertical axis of the sphere were determined using both approaches. The simplicity of the theory using the natural stress concept offers a good alternative for materials exhibiting linear relationship between natural strain and natural stress.

1. INTRODUCTION

IN A previous paper [1] the finite-strain field in a polyurethane rubber (Hysol 2085) sphere subjected to a series of increasingly larger diametral compression loads applied between two flat plates was determined using the embedded–moire technique. One of the two objects of the present paper is to determine the stresses for that same problem for which the strains were obtained.

Two approaches are followed to translate the experimentally determined strains into stresses. First the concept of strain–energy function for an isotropic, elastic body was used. Then, the stress field was determined with the Hookean type natural stress–natural strain relation developed by Parks and Durelli [2]. The concept of natural stress, analogous to the concept of natural strain, is defined as the integral of incremental stresses, each of them computed using the area corresponding to a particular incremental load level. For some materials, the natural stress–natural strain relation is linear up to high levels of strain.

The second object of this study is to compare the stress fields obtained from these two different methods in order to reassess the merit of each of them, especially since the latter method uses a very simple stress–strain relation which greatly simplifies the analysis.

Spheres are used in many industrial applications. Besides its academic interest the knowledge of stresses in spheres subjected to large deformations is of importance in the manufacturing of soft rollers.

2. DETERMINATION OF MATERIAL PROPERTIES

2.1 *Experiments*

Four specimens were made: one for uniaxial tensile, one for homogeneous equally biaxial tensile, one for strip-biaxial tensile and one for uniaxial compressive testing. The

† Research Assistant, Civil and Mechanical Engineering Department. The Catholic University of America.
‡ Professor, Civil and Mechanical Engineering Department. The Catholic University of America.

first three specimens were cut from a rubber sheet printed with $\frac{5}{8}$ in. × $\frac{5}{8}$ in. grids and routed to the shape and size shown in Figs. 1a, b, c and the last one was a casting of 1 in. × 1 in. × 2 in. on which $\frac{1}{4}$ in × $\frac{1}{4}$ in. grids were drawn (Fig. 1d).

For uniaxial tensile and compressive, and strip-biaxial tests, successively larger amounts of dead weights were applied to the specimens. In the compression test, the dry friction between the loading plates and specimen was decreased by applying grease. The grids were photographed after each step of loading. Deformations were obtained by analyzing the deformed grids. The measurements were made using a travelling microscope with a sensitivity of 0·00004 in.
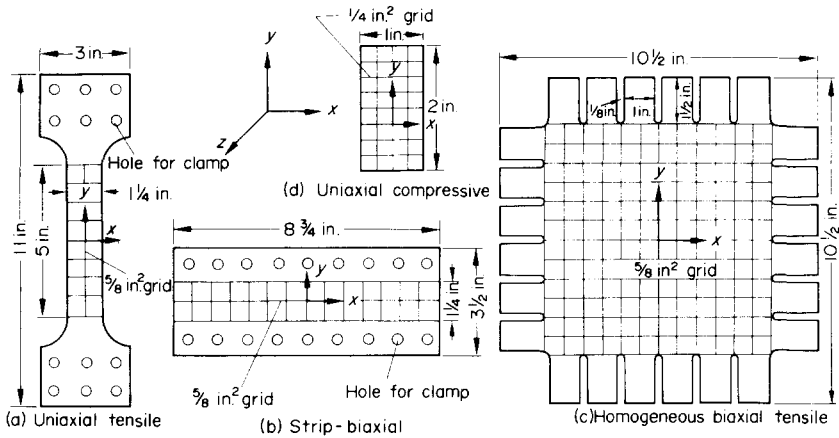
All specimens are 0·150 in. thick
but (d) which is 1 in. thick

FIG. 1.

The homogeneous equally biaxial tensile test was conducted using the loading frame shown in Fig. 2. By turning a pair of handles, force is transmitted to the specimen through metal wires. Turn-buckles permit small adjustments to equalize tension in the wires. Since the rubber of the sheet is birefringent, the uniformity of the distribution of the loading in each lug was verified by observing the photoelastic pattern. The forces applied were read from the pre-calibrated spring scales. The camera was placed vertically to photograph the specimen with the grids.

In the strip biaxial tensile test, the deformation in the transverse direction was prohibited to produce a biaxiality of two to one in stress when Hooke's law is obeyed and the material is incompressible, and close to that ratio of biaxiality when some departure of those conditions take place.

2.2 Elastic constants

The polyurethane rubber used for the experiment (100 PBW of Hysol 2085 and 45 PBW Hysol 3462) behaves like an incompressible material up to 300 per cent stretch in uniaxial tensile and down to 75 per cent in uniaxial compressive state of stress, and the natural Poisson's ratio ($\bar{\nu}$) is equal to 0·5 up to more than 100 per cent and down to about 27 per cent of natural strain (Fig. 3). The natural stress–natural strain relation is linear
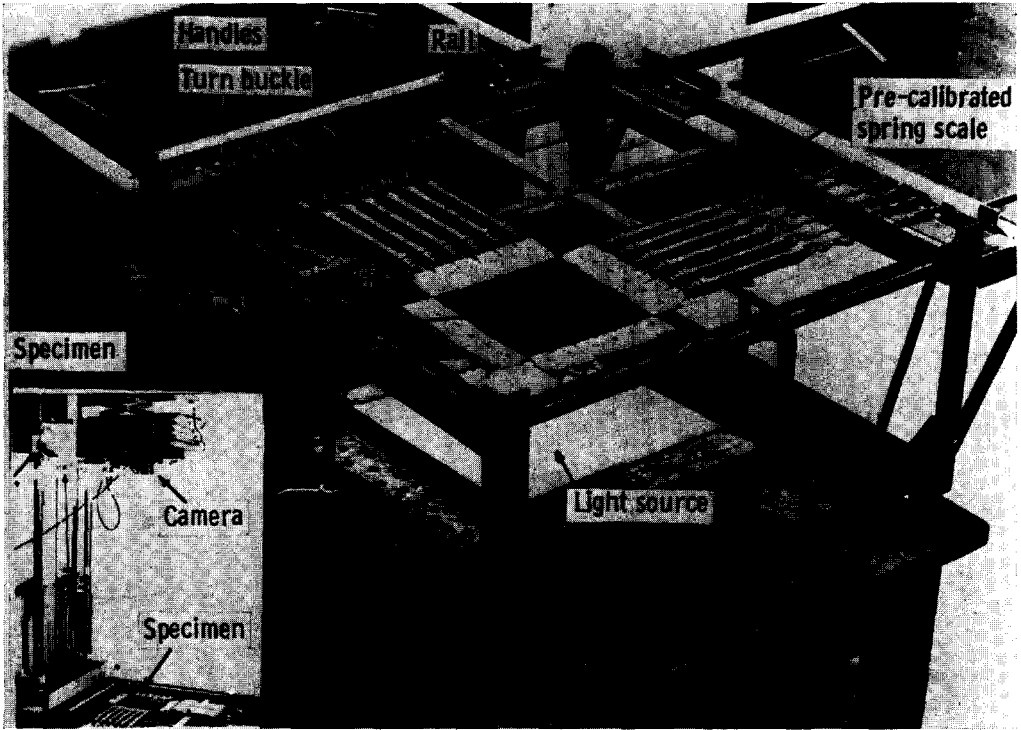
Fig. 2.
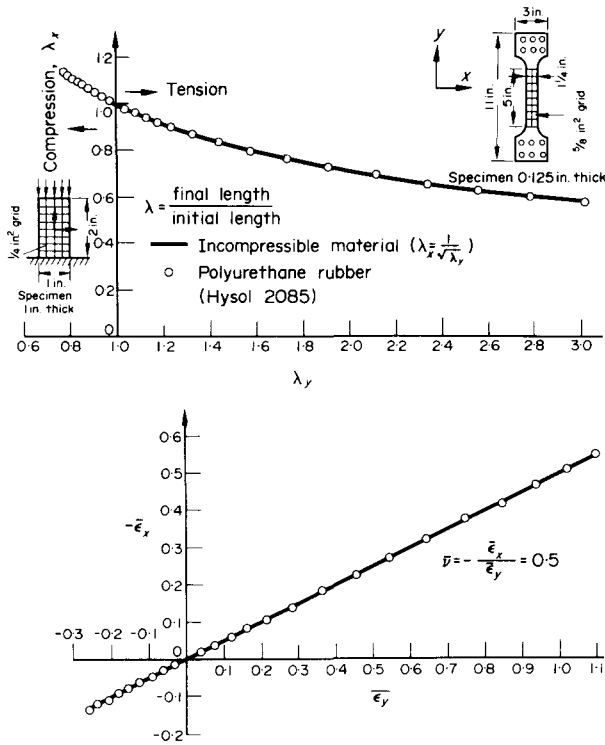
FIG. 3.

up to about 80 per cent tensile and 25 per cent compressive strain (Fig. 4). The natural modulus of elasticity ($\bar{E}$) determined from the natural stress–natural strain curve is 150 psi.

The principle of superposition can be applied to the biaxial state of stress and strain if natural stress and natural strain are considered [2]. With $\bar{E}$ and $\bar{v}$ obtained from the uniaxial test, the Hookean type of stress and strain relation is expressed by

$$\bar{\sigma}_x = \frac{\bar{E}}{1 - \bar{v}^2}(\bar{\varepsilon}_x + \bar{v}\bar{\varepsilon}_y). \tag{2.1}$$

A comparison of predicted stresses using equation (2.1) and experimentally determined stresses shows no deviation for the low values of natural strain and a maximum deviation of 5 per cent at 12 per cent natural strain for the homogeneous equally biaxial test and also 5 per cent at 17 per cent natural strain for the strip-biaxial test (Fig. 5).

The fact that the polyurethane rubber used in the investigation was incompressible imposes particular characteristics to the evaluation. As it is well known, when a material is incompressible, there is no way of computing three-dimensional stresses from the strains. It will be recalled that any amount of hydrostatic stress will produce no strain in such a material. The evaluation of stresses in this case is usually conducted by integrating the equations of equilibrium and eliminating the indeterminacy through known boundary values of stresses. This is the method that will be used in the paper but the reader should keep in mind that this limitation is imposed by the kind of material used in this particular case, and not by the stress analysis method.
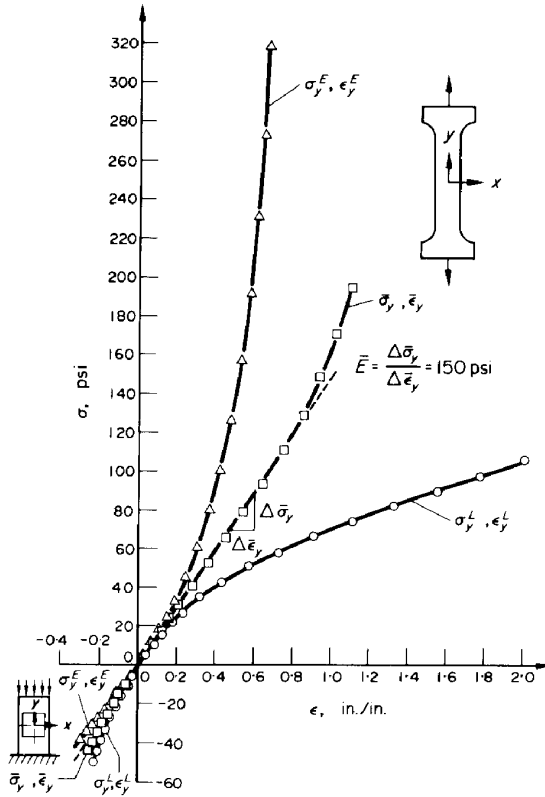
Fig. 4.

2.3 Strain energy function

For an incompressible, homogeneous and isotropic material, the strain–energy function W is a function of the two strain invariants I_1 and I_2 given by

$$I_1 = \lambda_1^2 + \lambda_2^2 + \lambda_3^2 = \lambda_1^2 + \lambda_2^2 + \frac{1}{\lambda_1^2 \lambda_2^2}$$

$$I_2 = \lambda_1^2 \lambda_2^2 + \lambda_2^2 \lambda_3^2 + \lambda_3^2 \lambda_1^2 = \lambda_1^2 \lambda_2^2 + \frac{1}{\lambda_1^2} + \frac{1}{\lambda_2^2}$$

(2.2a, b)

where λ_1, λ_2 and λ_3 are the principal stretches coinciding with the directions x, y and z in the calibration specimens of Fig. 1. The incompressibility is expressed by

$$I_3 = \lambda_1^2 \lambda_2^2 \lambda_3^2 = 1 \tag{2.2c}$$

which permitted the simplifications in the last equality of each of the equations (2.2a and b). For problems of plane stress, i.e. the stress σ_3^E coinciding with z direction vanishes, the
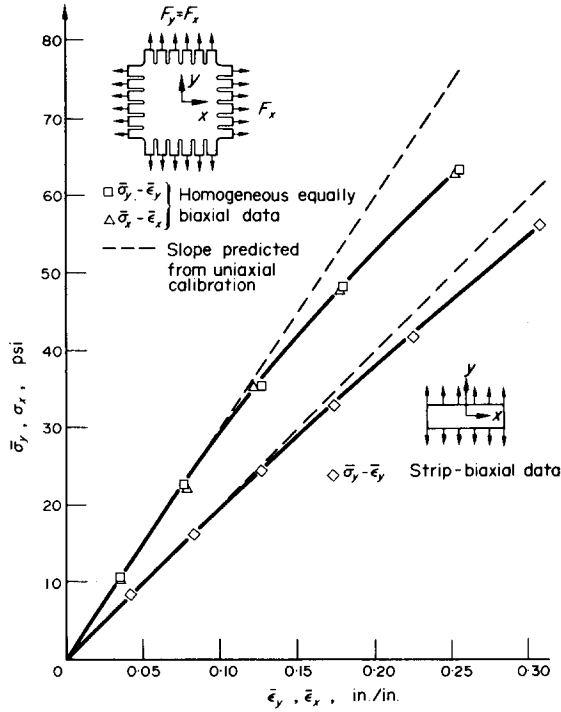
FIG. 5.

constitutive relation can be expressed as [3]

$$\sigma_1^E = 2\left(\lambda_1^2 - \frac{1}{\lambda_1^2\lambda_2^2}\right)\left(\frac{\partial W}{\partial I_1} + \lambda_2^2\frac{\partial W}{\partial I_2}\right)$$

$$\sigma_2^E = 2\left(\lambda_2^2 - \frac{1}{\lambda_2^2\lambda_1^2}\right)\left(\frac{\partial W}{\partial I_1} + \lambda_1^2\frac{\partial W}{\partial I_2}\right)$$

(2.3a, b)

where σ_1^E and σ_2^E are principal Eulerian stresses coinciding with x and y directions.

Gent and Thomas [4] have proposed the following mathematically simple form of strain energy function useful for some vulcanized rubbers

$$W = C_1(I_1 - 3) + C_2 \ln\left(\frac{I_2}{3}\right)$$

(2.4)

where C_1 and C_2 are constants. This form was found to fit well the experimental data of the polyurethane rubber used in the research reported in this paper.

To determine the values of C_1 and C_2, take the partial derivatives

$$\frac{\partial W}{\partial I_1} = C_1 \quad \text{and} \quad \frac{\partial W}{\partial I_2} = \frac{C_2}{I_2}$$

(2.5a, b)

from equation (2.4) and substitute them into equation (2.3a, b). Then

$$\sigma_1^E = 2\left(\lambda_1^2 - \frac{1}{\lambda_1^2 \lambda_2^2}\right)\left(C_1 + C_2 \frac{\lambda_2^2}{I_2}\right)$$

$$\sigma_2^E = 2\left(\lambda_2^2 - \frac{1}{\lambda_2^2 \lambda_1^2}\right)\left(C_1 + C_2 \frac{\lambda_1^2}{I_2}\right).$$

(2.6a, b)

Using the experimentally determined stresses and the corresponding stretches from uniaxial tensile and compressive, strip-biaxial and homogeneous equally biaxial tests and the above equations, the results were plotted the way shown in Fig. 6. Actually, the experimental data in the uniaxial tensile test alone would be sufficient to determine C_1 and C_2 [5]. The other test results provide additional verifications to the determination [6]. The data points are clustered around the straight line, the intercept and slope of which give the values of $C_1 = 17$ psi and $C_2 = 25$ psi, respectively. Thus the strain energy function W of the material used is

$$W = 17(I_1 - 3) + 25 \ln\left(\frac{I_2}{3}\right)$$

(2.7)

for $I_1 \leq 9.74$ and $I_2 \leq 6.14$ (range corresponding to the results of uniaxial tensile test). The highest values of strain invariants from the test on the sphere are $I_1 = 3.42$ and $I_2 = 3.55$ which fall within the range of calibration.

Young's modulus E which is the slope of the uniaxial stress–strain curve at zero strain was obtained by taking the partial derivative of σ_2^E with respect to λ_2 from equation (2.6b)
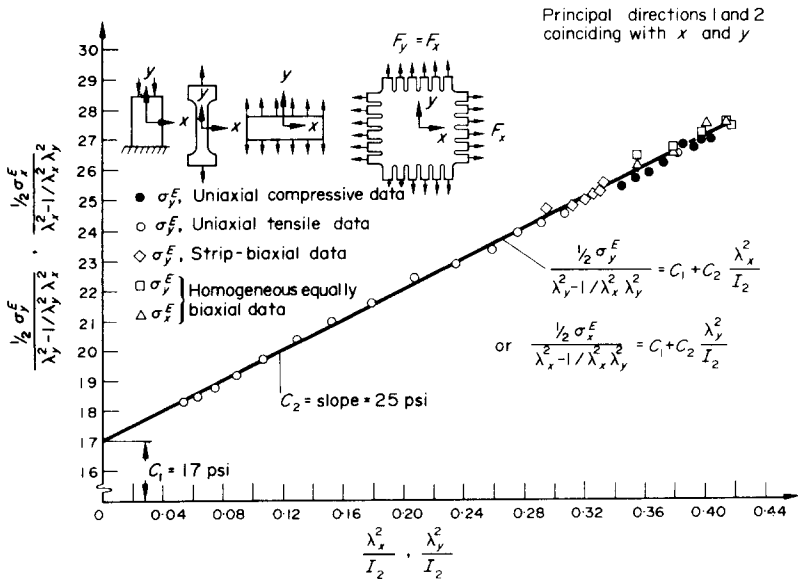

FIG. 6.

and using the relation $\lambda_1 = 1/\sqrt{\lambda_2}$

$$\left.\frac{\partial \sigma_2^E}{\partial \lambda_2}\right|_{\lambda_2 = 1} = 6C_1 + 2C_2 = 152 \text{ psi} \tag{2.8}$$

which is in agreement with the value obtained previously.

3. STRESS ANALYSIS AND RESULTS

The following methods of translating strain fields into stress field were used.

3.1 *Method of strain energy function*

Expressions for the stress components at a point of an incompressible body which is deformed in an arbitrary manner can be obtained by expanding the equation given in [7]. For a geometry and loading with rotational symmetry and using polar-cylindrical coordinates (u = radial displacement, $v = 0$ = tangential displacement, w = vertical displacement), these equations can be written in Eulerian description as

$$\sigma_{rr}^E = 2\left\{ \frac{\left(\frac{\partial u}{\partial z}\right)^2 + \left(1 - \frac{\partial w}{\partial z}\right)^2}{\left[\left(1 - \frac{\partial u}{\partial r}\right)\left(1 - \frac{\partial w}{\partial z}\right) - \frac{\partial u}{\partial z}\frac{\partial w}{\partial r}\right]^2} \frac{\partial W}{\partial I_2'} - \left[\left(1 - \frac{\partial u}{\partial r}\right)^2 + \left(\frac{\partial w}{\partial r}\right)^2\right]\frac{\partial W}{\partial I_1'} \right\} + p$$

$$\sigma_{\theta\theta}^E = 2\left\{ \frac{1}{(1-u/r)^2}\frac{\partial W}{\partial I_2'} - \left(1 - \frac{u}{r}\right)^2\frac{\partial W}{\partial I_1'} \right\} + p \tag{3.1a, b, c}$$

$$\sigma_{zz}^E = 2\left\{ \frac{\left(1 - \frac{\partial u}{\partial r}\right)^2 + \left(\frac{\partial w}{\partial r}\right)^2}{\left[\left(1 - \frac{\partial u}{\partial r}\right)\left(1 - \frac{\partial w}{\partial z}\right) - \frac{\partial u}{\partial z}\frac{\partial w}{\partial r}\right]^2} \frac{\partial W}{\partial I_2'} - \left[\left(\frac{\partial u}{\partial z}\right)^2 + \left(1 - \frac{\partial w}{\partial z}\right)^2\right]\frac{\partial W}{\partial I_1'} \right\} + p$$

and

$$\tau_{r\theta}^E = \tau_{\theta z}^E = 0$$

$$\tau_{rz}^E = 2\left[\left(1 - \frac{\partial u}{\partial r}\right)\frac{\partial u}{\partial z} + \frac{\partial w}{\partial r}\left(1 - \frac{\partial w}{\partial z}\right)\right]\left\{ \frac{\frac{\partial W}{\partial I_2'}}{\left[\left(1 - \frac{\partial u}{\partial r}\right)\left(1 - \frac{\partial w}{\partial r}\right) - \frac{\partial u}{\partial z}\frac{\partial w}{\partial r}\right]^2} + \frac{\partial W}{\partial I_1'} \right\} \tag{3.2a, b, c}$$

where p is an arbitrary hydrostatic pressure which is no longer equal to $\frac{1}{3}(\sigma_{rr}^E + \sigma_{\theta\theta}^E + \sigma_{zz}^E)$—the mean stress at the point—as in the infinitesimal theory of elasticity [8]. The strain

invariants are:

$$I'_1 = \left(1 - \frac{\partial u}{\partial r}\right)^2 + \left(\frac{\partial u}{\partial z}\right)^2 + \left(1 - \frac{u}{r}\right)^2 + \left(\frac{\partial w}{\partial z}\right)^2 + \left(1 - \frac{\partial w}{\partial z}\right)^2$$

$$I'_2 = \left(1 - \frac{u}{r}\right)^2 \left[\left(1 - \frac{\partial u}{\partial r}\right)^2 + \left(\frac{\partial u}{\partial z}\right)^2 + \left(\frac{\partial w}{\partial r}\right)^2 + \left(1 - \frac{\partial w}{\partial z}\right)^2\right]$$

$$+ \left[\left(1 - \frac{\partial u}{\partial r}\right)\left(1 - \frac{\partial w}{\partial z}\right) - \frac{\partial u}{\partial z}\frac{\partial w}{\partial r}\right]^2$$

$$I'_3 = \left(1 - \frac{u}{r}\right)^2 \left[\left(1 - \frac{\partial u}{\partial r}\right)\left(1 - \frac{\partial w}{\partial z}\right) - \frac{\partial u}{\partial z}\frac{\partial w}{\partial r}\right]^2.$$

(3.3a, b, c)

It is to be noted that the strain invariants used in these equations are given in terms of Cauchy's deformation tensor while those given in equations (2.2a, b, c) are in terms of Finger's. For an incompressible material, these invariants are related to each other by [9]

$$I_1 = I'_2, \qquad I_2 = I'_1, \qquad I_3 = I'_3 = 1$$

(3.4a, b, c)

and accordingly

$$\frac{\partial W}{\partial I'_1} = \frac{\partial W}{\partial I_2} = \frac{C_2}{I_2} = \frac{25}{I'_1}\text{psi}, \qquad \frac{\partial W}{\partial I'_2} = \frac{\partial W}{\partial I_1} = C_1 = 17\text{ psi}$$

(3.5a, b)

which are the values used in equations (3.1a, b, c and 3.2c).

Along the vertical and horizontal axes of the sphere, the cross spatial derivatives vanish and equations (3.1a, b, c) reduce to

$$\sigma^E_{rr} = 2\left[\frac{1}{(1 - \partial u/\partial r)^2}\frac{\partial W}{\partial I'_2} - \left(1 - \frac{\partial u}{\partial r}\right)^2\frac{\partial W}{\partial I'_1}\right] + p$$

$$= 2\left[\lambda^2_{rr}\frac{\partial W}{\partial I'_2} - \frac{1}{\lambda^2_{rr}}\frac{\partial W}{\partial I'_1}\right] + p$$

$$\sigma^E_{\theta\theta} = 2\left[\frac{1}{(1 - u/r)^2}\frac{\partial W}{\partial I'_2} - \left(1 - \frac{u}{r}\right)^2\frac{\partial W}{\partial I'_1}\right] + p$$

$$= 2\left[\lambda^2_{\theta\theta}\frac{\partial W}{\partial I'_2} - \frac{1}{\lambda^2_{\theta\theta}}\frac{\partial W}{\partial I'_1}\right] + p$$

(3.6a, b, c)

$$\sigma^E_{zz} = 2\left[\frac{1}{(1 - \partial w/\partial z)^2}\frac{\partial W}{\partial I'_2} - \left(1 - \frac{\partial w}{\partial z}\right)^2\frac{\partial W}{\partial I'_1}\right] + p$$

$$= 2\left[\lambda^2_{zz}\frac{\partial W}{\partial I'_2} - \frac{1}{\lambda^2_{zz}}\frac{\partial W}{\partial I'_1}\right] + p$$

where λ_{rr}, $\lambda_{\theta\theta}$ and λ_{zz} are principal stretches. Shear stresses vanish everywhere on the principal axes. Equations (3.3a, b, c) are also reduced to

$$I'_1 = \left(1 - \frac{\partial u}{\partial r}\right)^2 + \left(1 - \frac{u}{r}\right)^2 + \left(1 - \frac{\partial w}{\partial z}\right)^2$$

$$= \frac{1}{\lambda_{rr}^2} + \frac{1}{\lambda_{\theta\theta}^2} + \frac{1}{\lambda_{zz}^2}$$

$$I'_2 = \left(1 - \frac{\partial u}{\partial r}\right)^2 \left(1 - \frac{u}{r}\right)^2 + \left(1 - \frac{u}{r}\right)^2 \left(1 - \frac{\partial w}{\partial z}\right)^2 + \left(1 - \frac{\partial w}{\partial z}\right)^2 \left(1 - \frac{\partial u}{\partial r}\right)^2 \qquad (3.7a, b, c)$$

$$= \frac{1}{\lambda_{rr}^2 \lambda_{\theta\theta}^2} + \frac{1}{\lambda_{\theta\theta}^2 \lambda_{zz}^2} + \frac{1}{\lambda_{zz}^2 \lambda_{rr}^2}$$

$$I'_3 = \left(1 - \frac{\partial u}{\partial r}\right)^2 \left(1 - \frac{u}{r}\right)^2 \left(1 - \frac{\partial w}{\partial z}\right)^2$$

$$= \frac{1}{\lambda_{rr}^2 \lambda_{\theta\theta}^2 \lambda_{zz}^2}.$$

The stress component σ_{rr}^E along the horizontal axis was obtained by numerical integration along that axis using the equilibrium equation:

$$(\sigma_{rr}^E)_r = (\sigma_{rr}^E)_{r-\Delta r} - \sum \frac{\sigma_{rr}^E - \sigma_{\theta\theta}^E}{r} \Delta r - \sum \frac{\Delta \tau_{rz}^E}{\Delta z} \Delta r \qquad (3.8)$$

and remembering that at the boundary σ_{rr}^E is equal to zero. The terms $(\sigma_{rr}^E - \sigma_{\theta\theta}^E)$ and τ_{rz}^E were computed from equations (3.6a, b and 3.2c). The procedure is much the same as the shear-difference method of separation of stresses in photoelasticity. Except for the method used to determine the stresses the detailed procedure can be found in [10]. Once the radial stresses σ_{rr}^E along the horizontal axis are determined, the value of p at every point along the horizontal axis is obtained by subtracting the value of σ_{rr}^E from $(\sigma_{rr}^E - p)$, which is obtained from equation (3.6a). These values for p are substituted into equations (3.6b and c) to compute tangential and vertical stresses.

The stresses are shown normalized in Figs. 7, 8 and 9 by dividing them by the nominal stress

$$\sigma_p = \frac{P}{\pi R_0^2}$$

where R_0 is the original radius of sphere and P is the corresponding load.

To generalize the results the deformation of the sphere is characterized using a load parameter defined as

$$K = \frac{P}{\pi R_0^2 E} = \frac{\sigma_p}{E}$$

where E is Young's modulus obtained from equation (2.8). The results can then be applied to any sphere of any size provided the K value is the same. Alternatively, the deformation
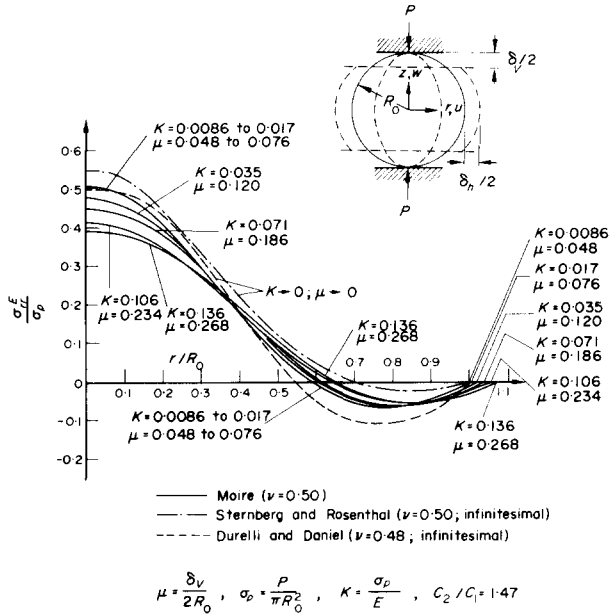
FIG. 7.

of the sphere can be characterized by using a deformation parameter

$$\mu = \frac{\delta_v}{2R_0} = \frac{\text{contraction of vertical axis}}{\text{dia. of sphere}}$$

Thus the results can also be used when μ values are known. Table 1 gives the values of μ, σ_p and K corresponding to P.
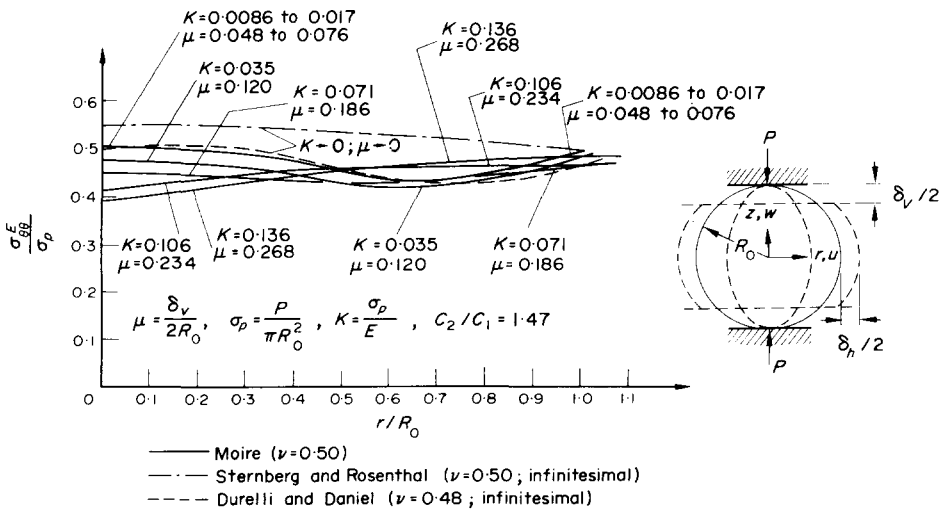

FIG. 8.

TABLE 1.

P (lb)	$\mu = \dfrac{\delta_v}{2R_0}$	$\sigma_p = \dfrac{P}{\pi R_0^2}$ (psi)	$K = \dfrac{\sigma_p}{E}$
48	0·048	1·30	0·0086
95	0·076	2·58	0·0170
195	0·120	5·29	0·035
395	0·186	10·72	0·071
595	0·234	16·15	0·106
760	0·268	20·62	0·136

In Fig. 9 the vertical stresses σ_{zz}^E for small deformations are compared to those obtained by Durelli and Daniel [11] and to the theoretical solution by Sternberg and Rosenthal [12]. Near the center the theoretical values are higher than those obtained here because the theory assumes point loading and in the experiments there is appreciable flattening at the poles.

All three normalized stresses near the center become smaller as the deformation becomes larger. The center of the sphere is a point of particular interest. Stresses and various definitions of strain at the center are plotted as a function of load in Fig. 10.
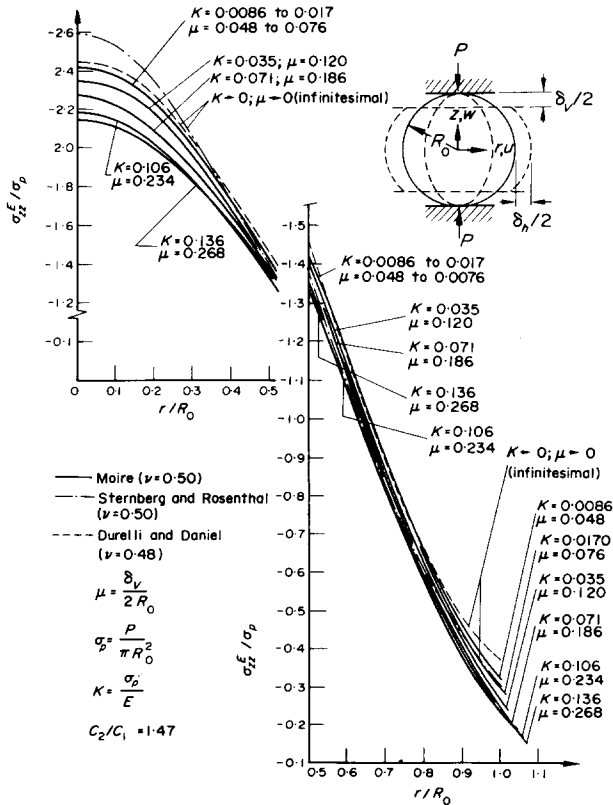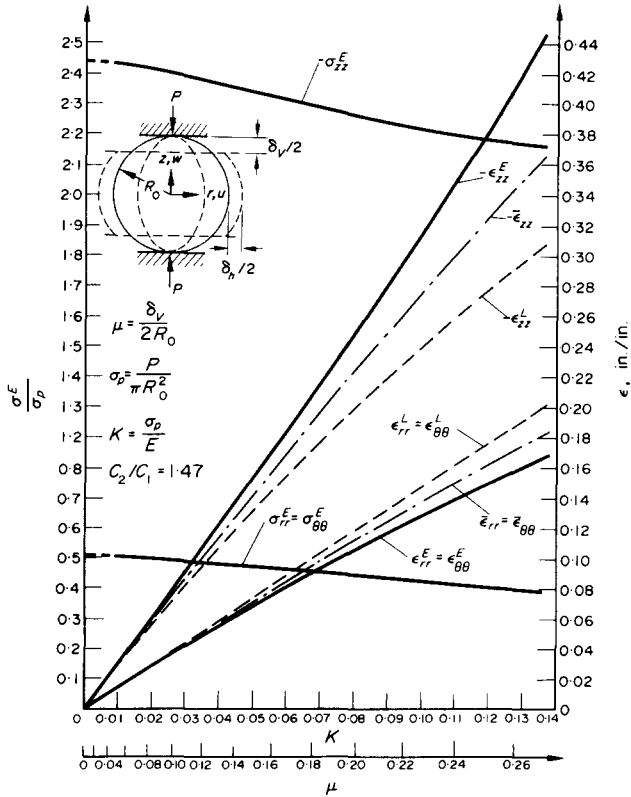

FIG. 9.

Fig. 10.

The procedure to evaluate stresses, described above, has also been applied to a line parallel to and $1\frac{1}{4}$ in. above the horizontal axis. It is to be noted, however, that the term $(\sigma_{rr}^E - \sigma_{\theta\theta}^E)$ was computed using general equations (3.1a, b). The results for one load level are shown in Fig. 11.

Equilibrium checks were made between the applied load and vertical stress on the equatorial plane for each load level and on the plane parallel to and $1\frac{1}{4}$ in. above it for one level of load. All agreements fall between $+3$ and -4.5 per cent.

The maximum shear stresses τ_{max}^E along the vertical axis of the sphere for several load levels are computed from the following equation:

$$\tau_{max}^E = \frac{|\sigma_{zz}^E - \sigma_{rr}^E|}{2} \tag{3.9}$$

and equations (3.6a and c). The results are shown in a normalized form in Fig. 12. For small deformation, the comparison with Frocht and Guernsey [13] is quite good. The values become progressively smaller as the deformations get larger.

The indeterminacy introduced into equations (3.1a, b, c) by the arbitrary hydrostatic pressure p can also be eliminated by expressing the constitutive relation in terms of the stress deviator, the only part of the stress that causes deformation. The stress deviator is
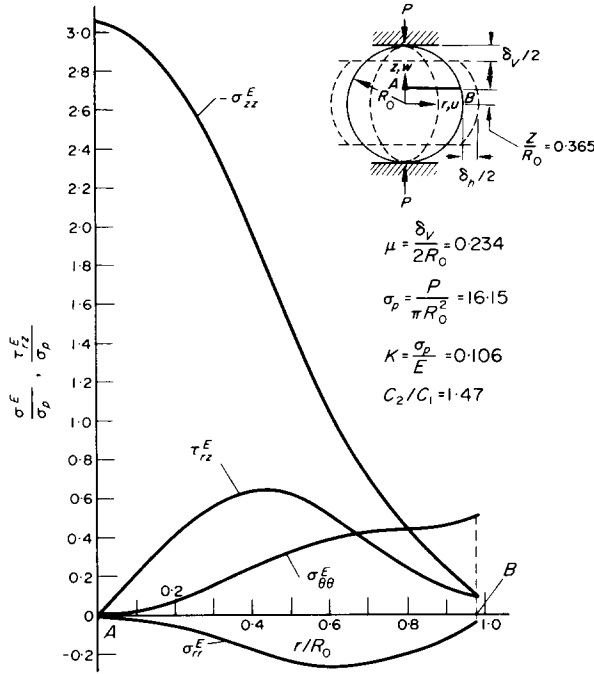
FIG. 11.

defined as

$$S_{ij} = \sigma_{ij} - \tfrac{1}{3}\delta_{ij}\sigma_{kk} \qquad (3.10)$$

where the indices $i, j = 1, 2, 3$ correspond to the radial, tangential and vertical directions. The deviatoric stresses so obtained along the horizontal axis for several load levels are shown in Figs. 13, 14 and 15. The results have not been normalized in these figures to emphasize the difference with natural stresses.

3.2 *Hooke's law in natural stress and natural strain*

The natural stress–natural strain relations in polar-cylindrical coordinates, along a principal axis are

$$\bar{\sigma}_{rr} = \frac{\bar{v}\bar{E}}{(1+\bar{v})(1-2\bar{v})}\bar{e} + \frac{\bar{E}}{1+\bar{v}}\bar{\varepsilon}_{rr}$$

$$\bar{\sigma}_{\theta\theta} = \frac{\bar{v}\bar{E}}{(1+\bar{v})(1-2\bar{v})}\bar{e} + \frac{\bar{E}}{1+\bar{v}}\bar{\varepsilon}_{\theta\theta} \qquad (3.11\mathrm{a,b,c})$$

$$\bar{\sigma}_{zz} = \frac{\bar{v}\bar{E}}{(1+\bar{v})(1-2\bar{v})}\bar{e} + \frac{\bar{E}}{1+\bar{v}}\bar{\varepsilon}_{zz}.$$

However, for an incompressible material

$$\bar{e} = \bar{\varepsilon}_{rr} + \bar{\varepsilon}_{\theta\theta} + \bar{\varepsilon}_{zz} = \ln(\lambda_{rr}\lambda_{\theta\theta}\lambda_{zz}) = 0$$

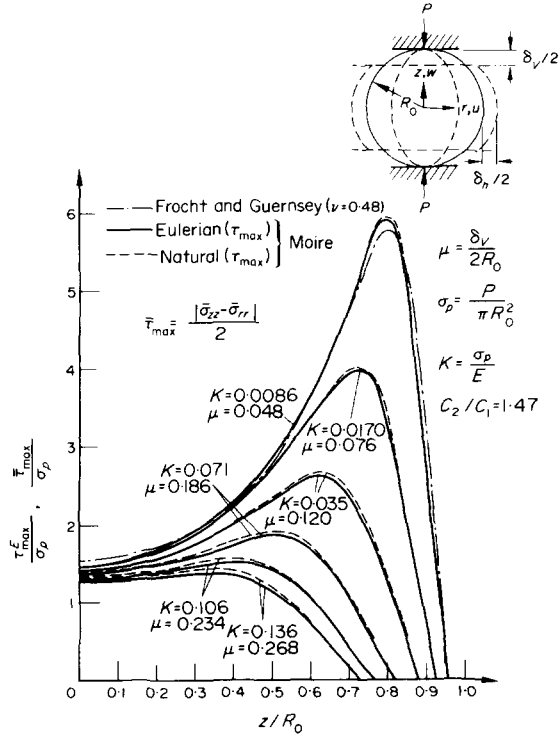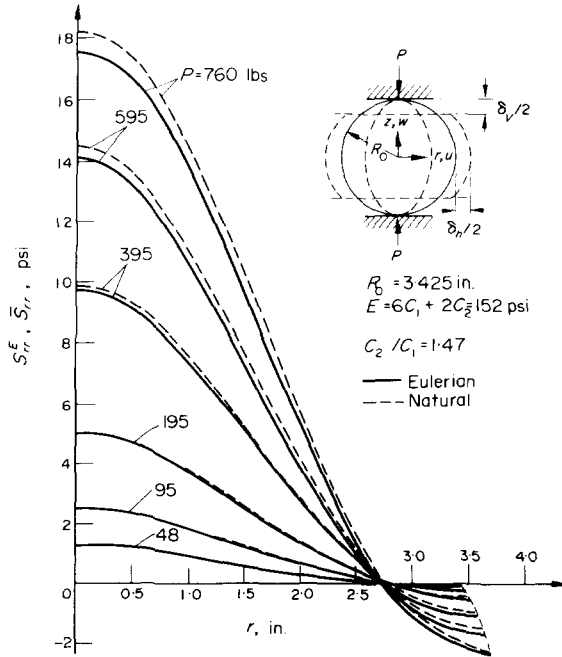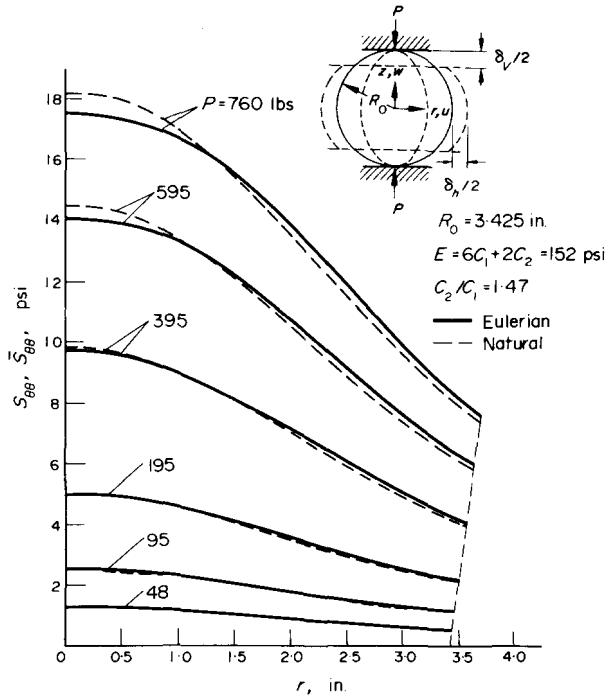Fig. 12.

Fig. 13.

FIG. 14.

and $1 - 2v$ is also equal to zero. Consequently, an indeterminacy arises. Call it $\bar{p}$, and equations (3.11a, b, c) can be written as

$$\bar{\sigma}_{rr} = \frac{\bar{E}}{1 + \bar{v}} \bar{\varepsilon}_{rr} + \bar{p}$$

$$\bar{\sigma}_{\theta\theta} = \frac{\bar{E}}{1 + \bar{v}} \bar{\varepsilon}_{\theta\theta} + \bar{p} \qquad (3.12a, b, c)$$

$$\bar{\sigma}_{zz} = \frac{\bar{E}}{1 + \bar{v}} \bar{\varepsilon}_{zz} + \bar{p}.$$

Sum up the above three equations and $\bar{p}$ is given by

$$\bar{p} = \tfrac{1}{3}(\bar{\sigma}_{rr} + \bar{\sigma}_{\theta\theta} + \bar{\sigma}_{zz}). \qquad (3.13)$$

Clearly, $\bar{p}$ is the mean stress at a point. Using equations (3.10 and 3.12a, b, c), the stress deviators are given by:

$$\bar{S}_{rr} = \frac{\bar{E}}{1 + \bar{v}} \bar{\varepsilon}_{rr}$$

$$\bar{S}_{\theta\theta} = \frac{\bar{E}}{1 + \bar{v}} \bar{\varepsilon}_{\theta\theta} \qquad (3.14a, b, c)$$

$$\bar{S}_{zz} = \frac{\bar{E}}{1 + \bar{v}} \bar{\varepsilon}_{zz}.$$

As pointed out the material used here obeyed Hookean type natural stress–natural strain relation up to 12 per cent in natural strain in homogeneous biaxial state of stress of equal ratio of biaxiality, and up to 80 per cent in uniaxial state of stress. These ranges allow the translation of all the natural strains obtained in the sphere into natural deviatoric stresses using equations (3.14a, b, c) and the previously determined material properties.

The deviatoric stresses on the horizontal axis are shown in Figs. 13, 14 and 15 and the normalized natural maximum shear stresses on the vertical axis in Fig. 12. The natural maximum shear stresses were obtained in a way similar to the Eulerian ones.
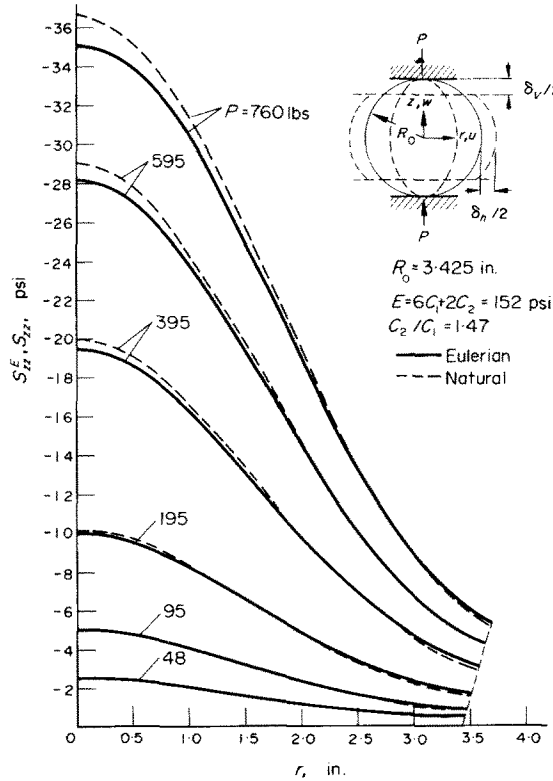

FIG. 15.

3.3 Deviatoric stresses obtained from both approaches

Since strictly speaking natural stresses do not satisfy equilibrium it would be difficult to determine the unknown hydrostatic pressure using natural stresses. The Eulerian and natural deviatoric stresses on the horizontal axis are not very different (see Figs. 13, 14 and 15). The most marked difference is noticeable for the vertical stress at the center of the sphere at the level $P = 760$ lb and is about 4·6 per cent. For small deformation, both approaches should degenerate to the linear stress–strain relation of infinitesimal elasticity and the results coincide as expected. The maximum shear stresses along the vertical axis obtained from the two approaches are also shown in Fig. 12.

4. CONCLUSIONS

The embedded-moire technique had been successfully applied to determine the interior state of stress and strain in a three-dimensional transparent body. The method gives whole-field information and makes possible the complete determination of the stress and strain tensors along an arbitrary line. This would have been very difficult, if not impossible, using any other of the presently available methods. The method is particularly suitable for finite-strain determinations.

Stress fields have been successfully obtained from strain fields using two approaches. The strain energy function approach has a well founded theoretical basis, yet the process is rather complex. On the other hand, the concept of natural stress offers a rather simple alternative.

Although the material used for the tests reported here is incompressible, the methods of analysis and the interpretation of the results obtained are not restricted to incompressible materials and apply equally well to any transparent material [14].

REFERENCES

[1] A. J. Durelli and T. L. Chen, Displacements and finite-strain fields in a sphere subjected to large deformations. Office of Naval Research Report No. 27, Civil and Mechanical Engineering Dept., Catholic Univ. of America, Feb. (1972). *Int. Non-linear Mech.* **8** (1), 17–30 (1973).
[2] V. J. Parks and A. J. Durelli, Natural stress. *Int. J. Non-linear Mech.* **4** (1), 7–16 (1969).
[3] R. S. Rivlin and D. W. Saunders, Large elastic deformation of isotropic materials—VII. Experiments on the deformation of rubber. *Phil. Trans.* **A243**, 251–288 (1951).
[4] A. N. Gent and A. G. Thomas, Forms for the stored (strain) energy function for vulcanized rubber. *J. Polymer Sci.* **28**, 626–628 (1958).
[5] P. B. Lindley, Plane-stress analysis of rubber at high strain using finite elements. *J. Strain Anal.* **6**, 45–52 (1971).
[6] P. J. Blatz and W. L. Ko, Application of finite elastic energy theory to the deformation of rubbery materials. *Trans. Soc. Rheol.* **6**, 223–251 (1962).
[7] A. C. Eringen, *Non-linear Theory of Continuous Media.* p. 156. McGraw-Hill, New York (1952).
[8] R. S. Rivlin, Large elastic deformations of isotropic material—I. Fundamental concepts. *Phil. Trans.* **A240**, 459–490 (1948).
[9] A. C. Eringen, *Non-linear Theory of Continuous Media.* p. 32. McGraw-Hill, New York (1962).
[10] A. J. Durelli, *Applied Stress Analysis.* p. 45. Prentice-Hall, N.J. (1967).
[11] A. J. Durelli and I. M. Daniel, A non-destructive three-dimensional strain analysis method. *J. appl. Mech. ASME,* **28**, 83–86 (1961).
[12] E. Sternberg and E. Rosenthal, The elastic sphere under concentrated loads. *J. appl. Mech.* **19**, *Trans. ASME,* 629–634 (1959).
[13] M. M. Frocht and R. Guernsey, Jr., A special investigation to develop a general method for three-dimensional photoelastic stress analysis. NACA Report 1148 (1953).
[14] A. J. Durelli, V. J. Parks and V. J. Lopardo, Stresses and finite strains around an elliptic hole in finite plate subjected to uniform load. *Int. J. Non-linear Mech.* **5**, 397–411 (1970).

Абстракт—Преобразовываются заранее определенные поля деформаций в шаре, подверженному действию больших деформаций, в поля напряжений, путем использования двух разных подходов к решению, а именно: функции энергим деформации и концепии естественного напряжения. Дается полное определение напряжений на экваториальной плоскости и параллельной к ее. Применяя два подхода к решению, определяются девиаторные напряжения на экваториальной плоскости и максимум напряжений сдвига вдоль вертикальной оси шара. Простота теории, которая использует концепцию естественного напряжения, является целесообразным вариантом для материалов, проявляющих линейную зависимость между естественной деформацией и естественным напряжением.